

MICROCOPY RESOLUTION TEST CHART
NBS 1963-A

Unclassified

SECURITY CLASSIFICATION OF THIS PAGE

REPORT DOCUMENTATION PAGE

1a. REPORT SECURITY CLASSIFICATION

Unclassified

1b. RESTRICTIVE MARKINGS

2a. SECURITY CLASSIFICATION AUTHORITY

3. DISTRIBUTION AVAILABILITY OF REP.
Approved for public release;
distribution is unlimited

2b. DECLASSIFICATION/DOWNGRADING SCHEDULE

4. PERFORMING ORGANIZATION REPORT NUMBER

FPO-1-77(29)

5. MONITORING ORGANIZATION REPORT #

6a. NAME OF PERFORM. ORG.

Ocean Engineering
& Construction
Project Office
CHESNAVFACENCOM

6b. OFFICE SYM

7a. NAME OF MONITORING ORGANIZATION

6c. ADDRESS (City, State, and Zip Code)

BLDG. 212, Washington Navy Yard
Washington, D.C. 20374-2121

7b. ADDRESS (City, State, and Zip)

8a. NAME OF FUNDING ORG.

8b. OFFICE SYM

9. PROCUREMENT INSTRUMENT INDENT #

8c. ADDRESS (City, State & Zip)

10. SOURCE OF FUNDING NUMBERS

PROGRAM	PROJECT	TASK	WORK UNIT
ELEMENT #	#	#	ACCESS #

11. TITLE (Including Security Classification)

Preliminary Analysis of Near-Field and Far-Field Arrays for Project Linear Chair

12. PERSONAL AUTHOR(S)

13a. TYPE OF REPORT

13b. TIME COVERED

FROM TO

14. DATE OF REP. (YYMMDD)

77-09

15. PAGES

51

16. SUPPLEMENTARY NOTATION

17. COSATI CODES

FIELD	GROUP	SUB-GROUP
-------	-------	-----------

18. SUBJECT TERMS (Continue on reverse if nec.)
Linear Chair, Dynamic analysis, Arrays,

19. ABSTRACT (Continue on reverse if necessary & identify by block number)
Project Linear Chair is examining methods of measuring the near field and far field magnetic, electric, and electro-magnetic signatures of various underwater platforms. Initial hydro-mechanical mooring approaches which have been proposed to position the sensor strings are depicted in Figure 1-1 for (Con't)

20. DISTRIBUTION/AVAILABILITY OF ABSTRACT
SAME AS RPT.

21. ABSTRACT SECURITY CLASSIFICATION

22a. NAME OF RESPONSIBLE INDIVIDUAL

Jacqueline B. Riley

DD FORM 1473, 84MAR

22b. TELEPHONE

202-433-3881

22c. OFFICE SYMBOL

SECURITY CLASSIFICATION OF THIS PAGE

BLOCK 19 (Con't)

the near field system and Figure 1-2 for the far field system.

A stringent requirement of any proposed mooring system is the movement of the attached sensors in response to ocean currents. A sensor watch circle of 3 ft. radius is a desired goal to achieve.



FPO-1-77(29)
SEPTEMBER 1977

PRELIMINARY ANALYSIS OF
NEAR-FIELD AND FAR-FIELD ARRAYS
FOR PROJECT LINEAR CHAIR

*Original contains color
plates: All DTIC reproductions
will be in black and
white*

PREPARED FOR
OCEAN ENGINEERING AND CONSTRUCTION PROJECT OFFICE
CHESAPEAKE DIVISION
NAVAL FACILITIES ENGINEERING COMMAND
WASHINGTON, D.C. 20374

TABLE OF CONTENTS

<u>Section</u>		<u>Page</u>
1	INTRODUCTION	1-1
	1.1 LINEAR CHAIR Requirements	1-1
	1.2 Overview of Report	1-1
2	NEAR-FIELD ARRAY ANALYSIS	2-1
	2.1 Configuration Discussion	2-1
	2.2 Results of Two-Buoy Configuration	2-4
	2.3 Results of Distributed Buoy Configuration	2-4
3	FAR-FIELD ARRAY ANALYSIS (GOAL POST)	3-1
	3.1 Overview	3-1
	3.2 Analysis Approach	3-1
	3.3 Basic Configuration	3-3
	3.4 Analysis of Vertical Strings	3-3
	3.5 Determine Resultant Force on Trapezoid	3-10
	3.6 Analysis of the Trapezoid	3-10
	3.7 Observation of Far-Field Goal Post Analysis	3-17

APPENDICES

A	CALCULATIONS OF SPHERICAL BUOY PARAMETERS	A-1
B	APPLICATION OF NEWTON'S METHOD IN CALCULATING THE EQUILIBRIUM CONFIGURATION OF A TWO-LEGGED BUOY MOORING WITH AN IN-PLANE CURRENT	B-1

Accession For	
NTIS CRA&i	<input checked="" type="checkbox"/>
DTIC TAB	<input type="checkbox"/>
Unannounced	<input type="checkbox"/>
Justification	
By	
Distribution /	
Availability Codes	
Dist	Avail and/or Special
A-1	

LIST OF ILLUSTRATIONS

<u>Figure</u>		<u>Page</u>
1-1	Candidate Mooring Configurations for the Near-Field Array System	1-2
1-2	Candidate Mooring Configuration for the Far-Field Array System	1-3
2-1	Two-Buoy Near-Field Array Analysis Diagram	2-2
2-2	Distributed Buoy Near-Field Array Analysis Diagram	2-3
2-3	Distributed Buoy Watch Circle Comparisons	2-9
3-1	Far-Field Goal Post Array Analysis Diagram	3-2
3-2	Equilibrium Diagram for the Trapezoidal Array With Zero Current	3-4
3-3	Vertical Strings Analysis Diagram	3-5
3-4	Preliminary Watch Circle Trade-Offs of Vertical Sensor Strings	3-6
3-5	Vector Force Diagram for Determining Resultant Force on Trapezoid Apex	3-11
3-6	Intuitive Response Geometry to a Planar Current for the Goal Post Array	3-12
3-7	Goal Post Array Response to a 1-knot Plan Current	3-16
B-1	Trapezoidal Array Nomenclature	B-2

LIST OF TABLES

<u>Table</u>		<u>Page</u>
2-1	Configuration Parameters for Near-Field Array Analysis	2-1
2-2	Watch Circle Radii (Feet) with 500 Pounds Net Buoyancy at the Top for Various Intermediate Position Buoyancies and Currents	2-5
2-3	Watch Circle Radii with 1000 Pounds Net Buoyancy at the Top for Various Intermediate Position Buoyancies and Uniform Currents	2-6
2-4	Watch Circle Radii with 3000 Pounds Net Buoyancy at the Top for Various Intermediate Position and Uniform Currents	2-7
2-5	Watch Circle Radii with 5000 Pounds Net Buoyancy at the Top for Various Intermediate Position and Uniform Currents	2-8
3-1	Geometric Response for Vertical Strings for Various Combinations of Buoyancy, Cable Diameter, and Uniform Current	3-7
A-1	Net Buoyancy and Buoy Diameter	A-3
A-2	Spherical Buoy Drag, lbs	A-4

Section 1

INTRODUCTION

1.1 LINEAR CHAIR REQUIREMENTS

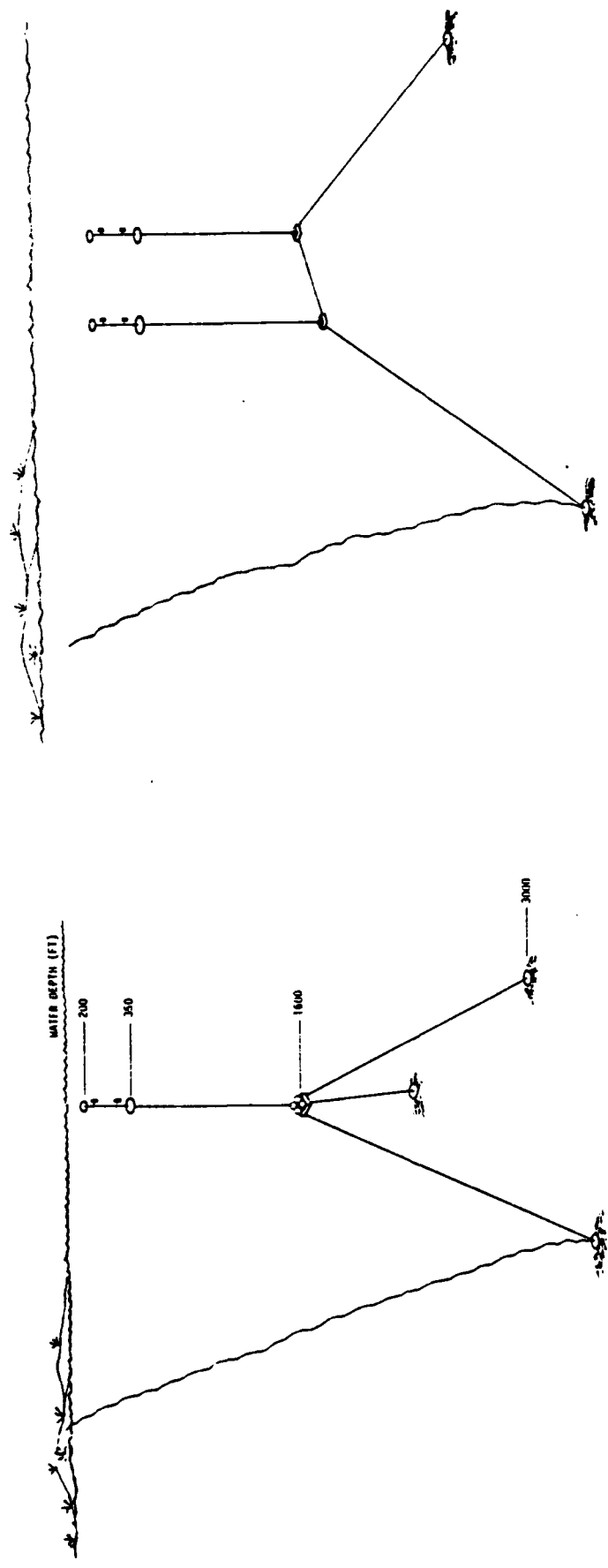
Project Linear Chair is examining methods of measuring the near field and far field magnetic, electric, and electro-magnetic signatures of various underwater platforms. Initial hydro-mechanical mooring approaches which have been proposed to position the sensor strings are depicted in ~~Figure 1-1~~ for the near field system and ~~Figure 1-2~~ for the far field system.

A stringent requirement of any proposed mooring system is the movement of the attached sensors in response to ocean currents. A sensor watch circle of 3 ft. radius is a desired goal to achieve.

1.2 OVERVIEW OF REPORT

The following report contains analysis methods for determining the static deflections that could be expected from the mooring configurations depicted in Figures 1-1 and 1-2. The analysis methods have been exercised for various parametric combinations of system components to obtain an initial range of excursions that could be expected under different current conditions. It is emphasized that these initial results are primarily presented for illustrative purposes since gross assumptions were made concerning the size and weight of system components. However, as the specific designs are evolved, the analysis techniques presented herein can serve as a valuable design tool to assess the hydro-mechanical performance to be expected.

Section 2 addresses the near field array analysis and Section 3 addresses the far field (goal post) array analysis. Appendices have been used liberally to present detailed mathematical formulations and descriptions for those readers who are interested.



GOAL POST ARRAY

TRI-MOOR ARRAY

Figure 1-1. Candidate Mooring Configurations for the Near-Field Array System

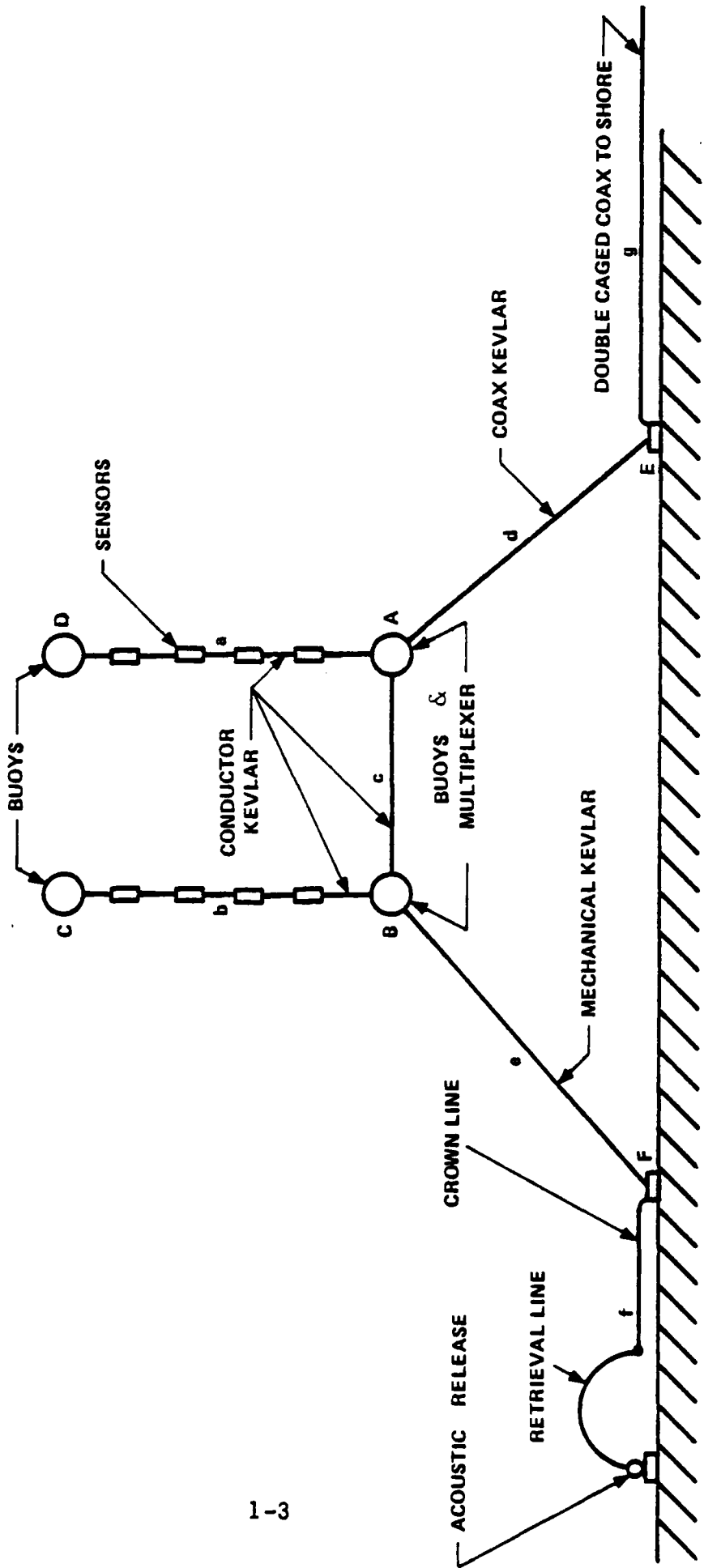


Figure 1-2. Candidate Mooring Configuration for the Far-Field Array System

Section 2

NEAR-FIELD ARRAY ANALYSIS

2.1 CONFIGURATION DISCUSSION

The proposed near field array consists of two independent sensor strings separated by approximately 180 ft. Table 2-1 contains the pertinent parameters examined in this analysis.

Table 2-1. Configuration Parameters for Near-Field Array Analysis

Water Depth	3000 ft.
Cable Parameters	
Construction	Kevlar
Diameters	0.3, 0.5, and 1.0 inches
Overall length	2600 ft.
Buoyed length	1000 ft.
Wt/ft. (water)	0 (neutrally buoyant)
Buoy Parameters	
Material	Aluminum 6061-T6
Net Buoyancies	500, 1000, 3000, 5000 lbs. with
Diameters	of 3.02, 3.80, 5.49, 6.51 ft. respectfully
Shape	Spherical
Drag Coefficient	0.5 based on frontal area
Currents	
Type	Uniform for entire depth
Magnitude	0.05, 0.1, 0.3, 0.5, and 1.0 kts.

The buoy parameters were calculated based on a 3000 ft. design depth and a safety factor of 3. Detailed calculations of the buoy parameters are contained in Appendix A.

The configurations analyzed were of two types and are depicted in Figures 2-1 and 2-2. In the two-buoy configurations the size of the buoy at the top and intermediate positions were sequentially changed. The resultant

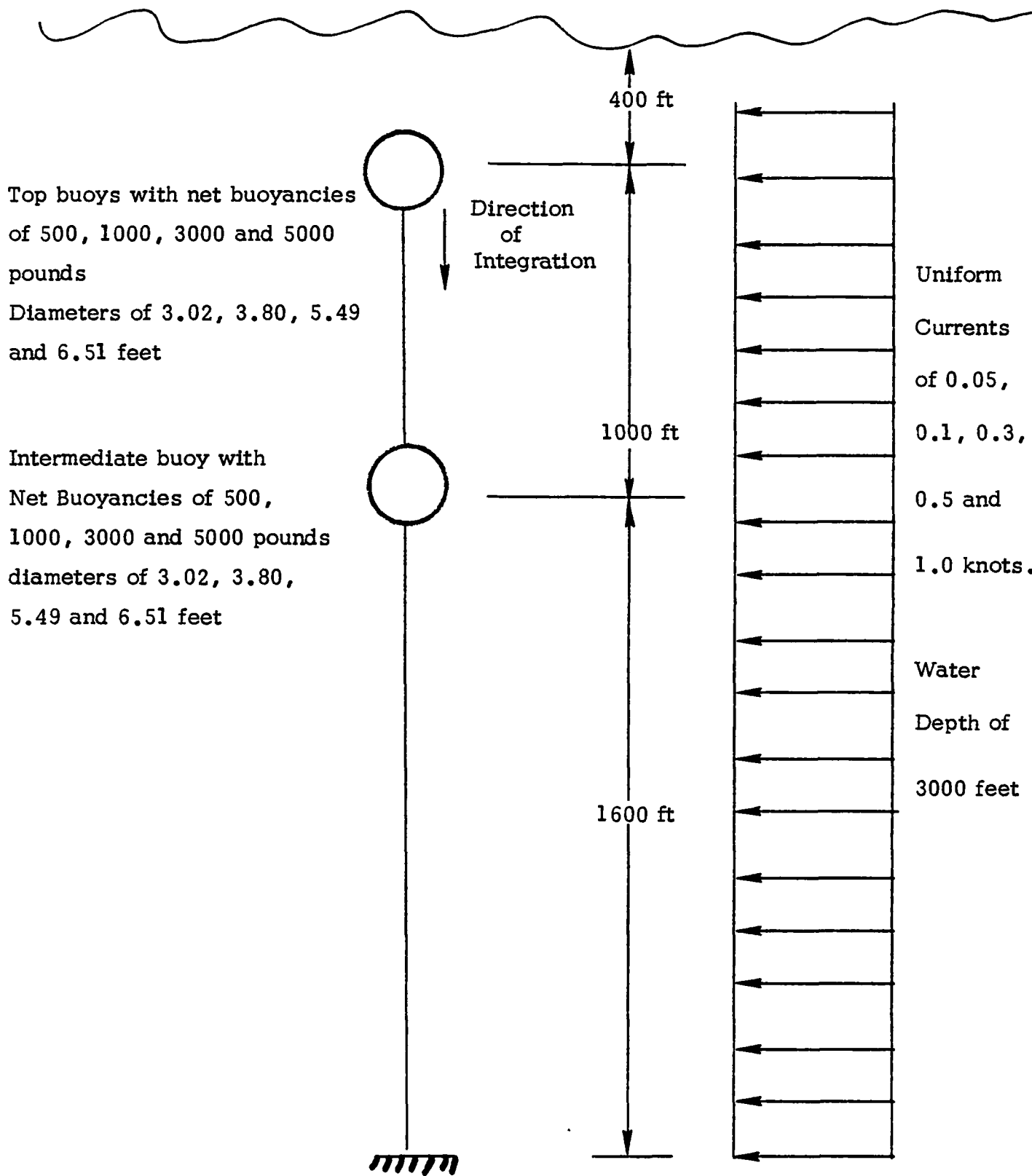


Figure 2-1. Two-Buoy Near-Field Array Analysis Diagram

All buoys have 500 pounds
Net Buoyancy with 3.02 foot
diameter

0.5 inch Smooth Neutrally
Buoyant Kevlar Cable

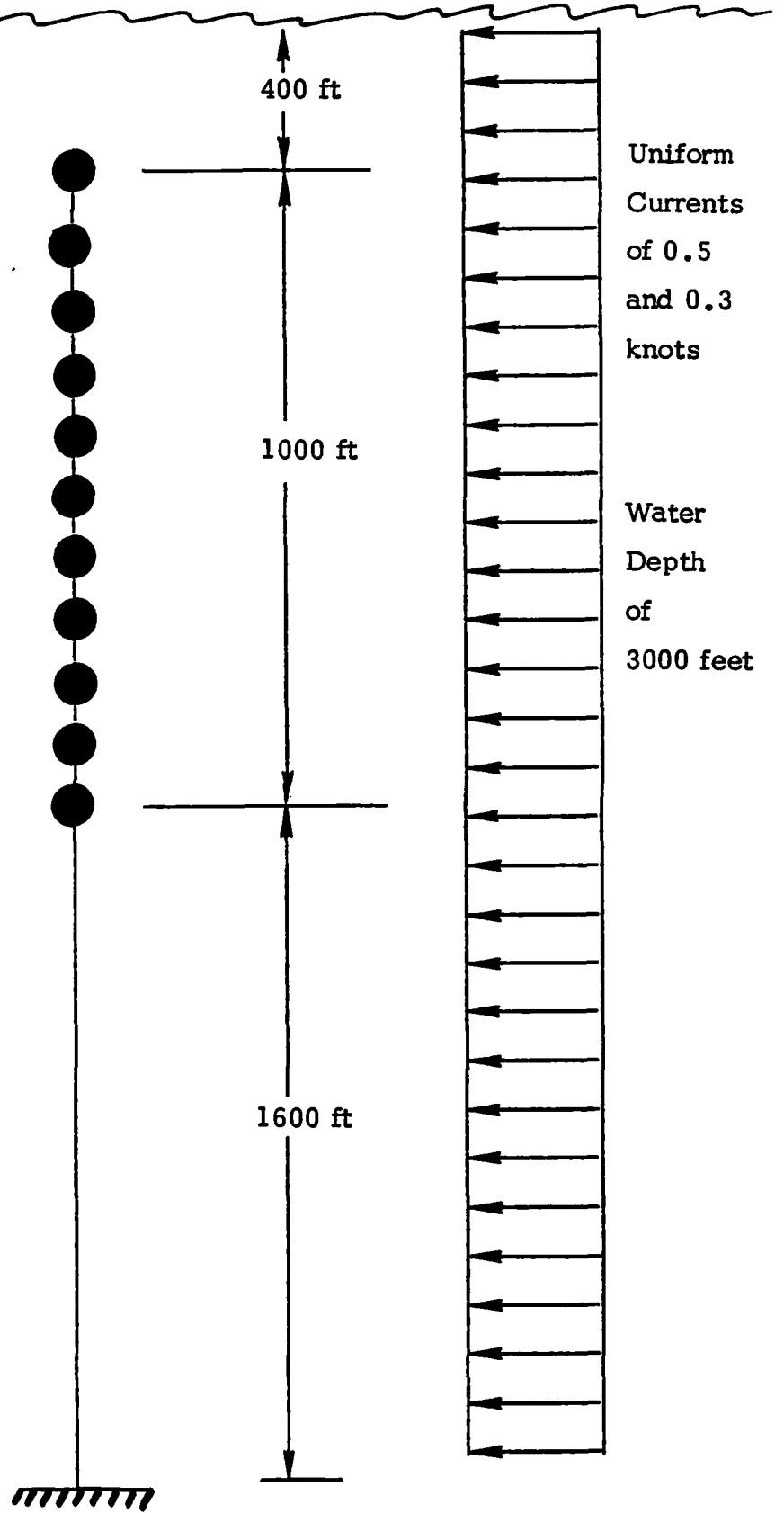


Figure 2-2. Distributed Buoy Near-Field Array Analysis Diagram

configurations were then analyzed in uniform currents of 0.05, 0.1, 0.3, 0.5, and 1.0 knots. In the distributed buoy configuration 11 500-lb. buoys were uniformly spaced over the 1000-ft. buoyed length. This configuration was analyzed in currents of 0.3 and 0.5 knots.

2.2 RESULTS OF TWO-BUOY CONFIGURATION

Tables 2-2 thru 2-5 contain the computed watch circle radii for the top and intermediate buoy under different configurations and currents. The tables are for net buoyancies of 500, 1000, 3000, and 5000 lb at the top, respectively.

The combinations that satisfy the initial watch circle radius of 3 ft. for the top buoy are delineated by the red line in the tables.

2.3 RESULTS OF DISTRIBUTED BUOY CONFIGURATION

In addition to examining a two buoy approach, uniformly distributed loading of the top 1000 feet of the cable was also investigated. The following parameters were used:

Cable	
Diameter	0.5 inch
Wt/ft. (water)	0 (neutrally buoyant)
Buoy	
Net Buoyancy	500 lbs.
Diameter	3.02 ft.
Number	11 buoys uniformly spaced over top 1000 ft. scope.
Current	
Type	Uniform
Magnitude	0.3, 0.5 knots.

The intent of examining the uniformly spaced buoyancy was to obtain tradeoffs in watch circle performance for distributed versus concentrated buoyancy elements in a uniform current. The cases compared are depicted graphically in Figure 2-3. The composite net buoyancy in each system

Table 2-2. Watch Circle Rad11 (Feet) with 500 Pounds Net Buoyancy at the Top For Various Intermediate Position Buoyancies and Currents

CURRENT KNOTS	CABLE DIAMETER INCHES	INTERMEDIATE NET BUOYANCY											
		500 lb		1000 lb		3000 lb		5000 lb		5000 lb		5000 lb	
		TOP BUOY	INT BUOY	TOP BUOY	INT BUOY	TOP BUOY	INT BUOY	TOP BUOY	INT BUOY	TOP BUOY	INT BUOY	TOP BUOY	INT BUOY
.05	.3	1.04	.81	0.78	0.55	.47	0.24	.40	0.17				
	.5	1.43	1.20	1.04	0.58	0.58	0.35	0.47	0.24				
.1	1.0	2.40	2.17	1.69	1.46	0.86	0.63	0.65	0.42				
	.3	2.23	2.02	2.05	1.84	1.02	0.81	0.80	0.59				
.3	.5	3.37	3.16	2.38	2.17	1.46	1.25	1.08	0.87				
	1.0	6.21	6.00	4.27	4.26	1.97	1.76	1.79	1.58				
.5	.3	30.43	23.81	19.70	13.12	12.30	5.68	10.91	4.29				
	.5	54.71	41.66	39.20	26.15	21.65	18.60	19.20	6.15				
.5	1.0	115.79	86.84	85.27	56.32	49.85	20.90	39.73	10.78				
	.3	103.90	76.99	77.34	50.43	45.50	18.59	38.81	16.10				
1.0	.5	171.86	127.39	28.74	84.27	76.59	32.12	65.09	20.62				
	1.0	340.19	251.86	256.26	167.93	156.51	68.18	131.38	43.05				
1.0	.3	444.07	323.55	341.78	221.26	213.74	93.22	184.54	64.02				
	.5	691.47	503.90	535.32	347.75	336.08	148.51	286.82	99.25				
1.0	1.0	1182.49	847.90	948.06	613.57	606.99	272.60	512.61	178.22				

Table 2-3. Watch Circle Rad11 with 1000 Pounds Net Buoyancy at the Top for Various Intermediate Position Buoyancies and Uniform Currents

CURRENT KNOTS	CABLE DIAMETER INCHES	INTERMEDIATE NET BUOYANCY											
		500 lb		1000 lb		3000 lb		5000 lb					
		TOP BUOY	INT BUOY	TOP BUOY	INT BUOY	TOP BUOY	INT BUOY	TOP BUOY	INT BUOY				
.05	.3	.50	.46	.40	.36	.22	.18	.18	.14				
	.5	.76	.72	.59	.55	.32	.28	.24	.20				
	1.0	1.41	1.37	1.08	1.04	.57	.53	.41	.37				
	.3	2.00	1.84	1.59	1.43	.90	.74	.72	.56				
	.5	2.34	2.18	2.37	2.21	1.29	1.13	.98	.82				
.3	1.0	4.23	4.07	3.26	3.10	2.26	2.10	1.63	1.47				
	.3	14.55	13.09	11.45	9.99	6.64	5.18	5.54	4.08				
	.5	31.36	26.16	23.77	18.57	12.94	7.74	10.98	5.78				
	1.0	69.04	56.36	53.73	41.05	30.26	17.50	22.71	10.03				
	.5	63.25	50.47	49.95	37.17	28.13	15.35	24.10	11.32				
1.0	.5	105.88	84.38	84.31	62.81	49.95	28.45	40.00	18.50				
	1.0	211.88	168.45	169.15	125.72	103.46	60.03	82.92	39.49				
	.3	286.52	222.19	231.47	170.14	148.01	83.68	124.50	60.17				
	.5	450.91	351.69	368.13	269.68	232.87	133.65	192.90	93.68				
	1.0	821.59	637.96	681.92	498.29	438.50	254.87	358.44	171.81				

Table 2-4. Watch Circle Radii with 3000 Pounds Net Buoyancy at the Top for Various Intermediate Position Buoyancies and Uniform Currents

CURRENT KNOTS	CABLE DIAMETER INCHES	INTERMEDIATE NET BUOYANCY											
		500 lb		1000 lb		3000 lb		5000 lb		5000 lb		5000 lb	
		TOP BUOY	INT BUOY	TOP BUOY	INT BUOY	TOP BUOY	INT BUOY	TOP BUOY	INT BUOY	TOP BUOY	INT BUOY	TOP BUOY	INT BUOY
.05	.3	.25	.22	.22	.19	.16	.13	.11					
	.5	.36	.33	.29	.23	.20	.16	.16					
	1.0	.64	.61	.54	.39	.36	.31	.28					
	.3	.98	.87	.79	.65	.54	.57	.46					
	.5	1.43	1.32	1.18	.91	.76	.80	.65					
.3	1.0	1.94	1.83	2.26	2.15	1.56	1.45	1.14					
	.3	7.19	6.08	6.63	5.02	4.88	3.87	3.37					
	.5	10.11	9.10	9.19	8.18	6.59	5.58	4.65					
	1.0	23.06	21.44	19.65	18.03	11.45	9.83	7.84					
	.5	22.82	20.01	19.39	16.58	13.57	10.76	9.36					
1.0	.5	39.64	33.6	35.74	29.70	24.00	17.96	12.91					
	1.0	82.68	70.01	74.02	61.35	51.67	39.00	28.75					
	.3	123.91	99.61	113.04	88.78	82.39	58.09	46.86					
	.5	193.05	157.21	174.93	139.09	127.78	91.94	72.45					
	1.0	363.90	298.67	328.86	263.63	241.05	175.82	135.19					

Table 2-5. Watch Circle Rad11 with 5000 Pounds Net Buoyancy at the Top for Various Intermediate Position Buoyancies and Uniform Currents

CURRENT KNOTS	CABLE DIAMETER INCHES	INTERMEDIATE NET BUOYANCY											
		500 lb			1000 lb			3000 lb			5000 lb		
		TOP BUOY	INT BUOY	TOP BUOY	INT BUOY	TOP BUOY	INT BUOY	TOP BUOY	INT BUOY	TOP BUOY	INT BUOY	TOP BUOY	INT BUOY
.05	.3	.17	.15	.16	.14	.13	.11	.12	.10				
	.5	.24	.22	.23	.21	.18	.16	.16	.14				
	1.0	.42	.40	.39	.37	.30	.28	.26	.24				
	.3	.69	.60	.65	.56	.52	.41	.48	.37				
	.5	.97	.86	.91	.82	.72	.63	.64	.55				
.3	1.0	1.68	1.59	1.57	1.48	1.21	1.12	1.03	.94				
	.3	5.14	4.29	4.93	4.08	4.00	3.15	4.32	3.42				
	.5	7.00	6.15	6.63	5.78	5.28	4.43	4.77	3.92				
	1.0	11.65	10.80	10.89	10.04	8.48	7.63	7.32	6.47				
	.3	14.29	11.92	13.69	11.32	11.12	8.75	10.40	8.03				
.5	.5	23.05	20.68	20.89	18.52	14.67	12.3	13.24	10.87				
	1.0	50.10	43.37	46.31	39.58	34.88	28.15	29.42	22.69				
	.3	79.97	64.60	75.72	60.35	59.80	44.43	54.1	38.73				
	.5	124.12	101.57	116.78	94.23	92.62	70.07	81.09	58.54				
	1.0	233.10	193.13	218.19	178.22	172.93	132.76	147.24	109.27				

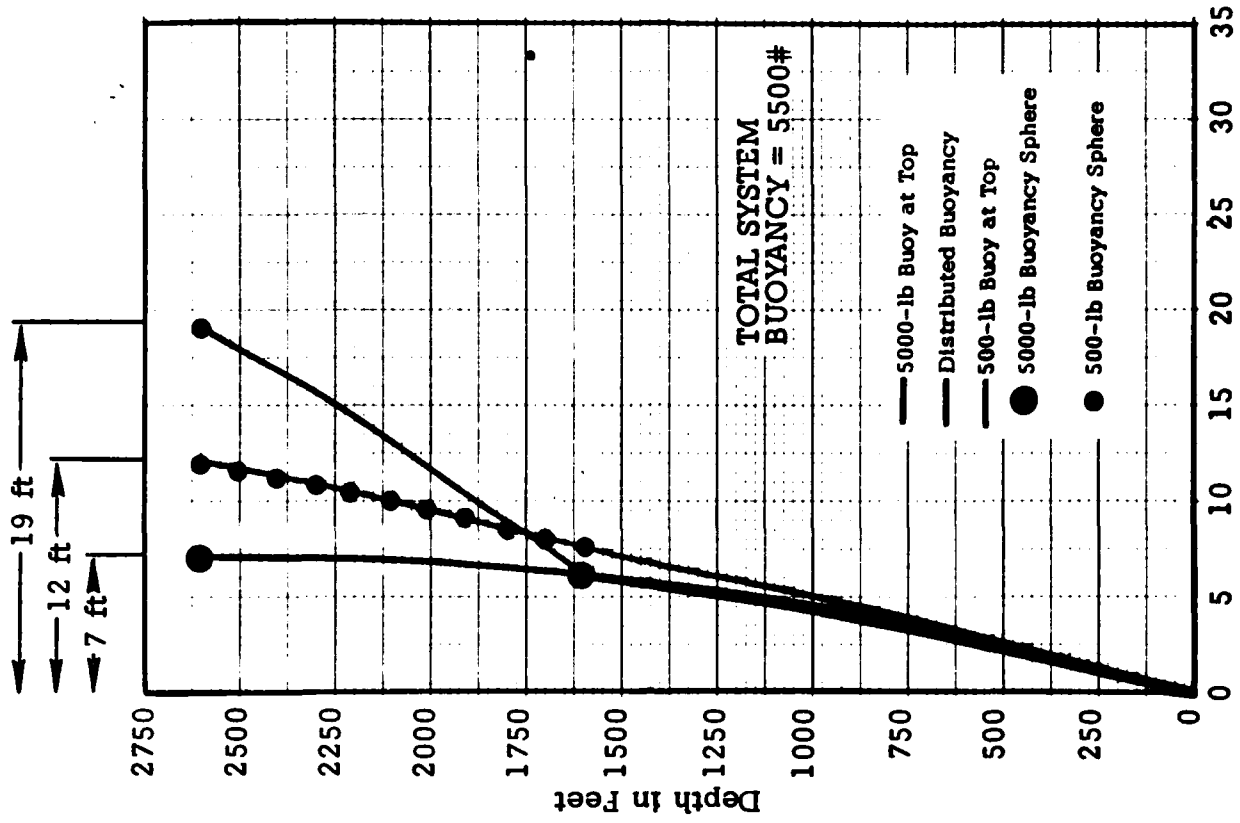
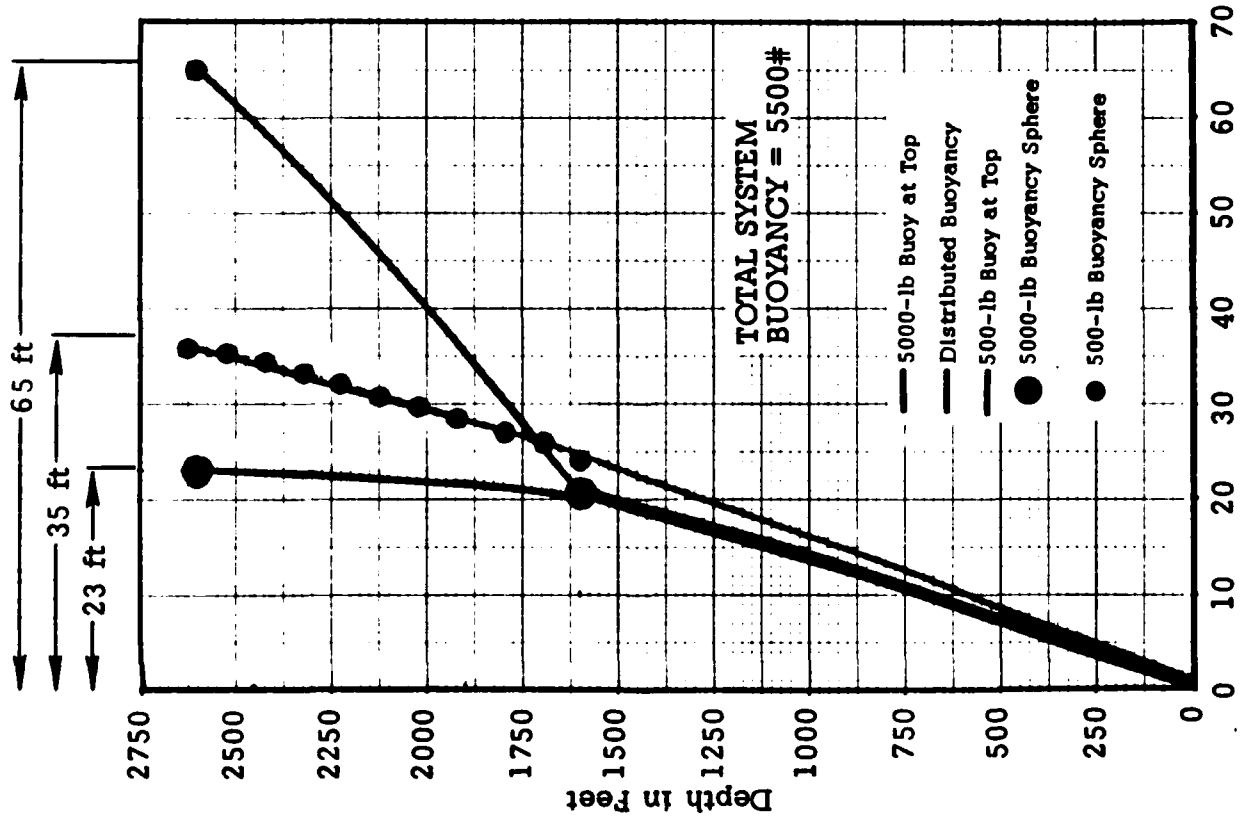


Figure 2-3. Distributed Buoy Watch Circle Comparisons

compared totaled 5500 lb. As observed in the data, the two-buoy system with the larger (5000-lb) buoy at the top results in the better watch circle performance when the configuration is exposed to a uniform current. This result is generally true for uniform currents; however, for sharp current profiles, a distributed buoyancy approach is generally better because the buoys are placed in lower currents and thus result in reduced system drag. When current data from specific sites are known, more meaningful tradeoffs can be made.

Section 3

FAR-FIELD ARRAY ANALYSIS (GOAL POST)

3.1 OVERVIEW

The goal post array, in the analytical sense, represents a system which must be analyzed in an iterative fashion. Figure 3-1 depicts the configuration which has been examined. The intent has been to obtain a technique that can determine the absolute current response of various system components relative to a zero current condition. For the material presented herein the current has been assumed to be uniform and planar; however, the technique can easily be extended to cover currents at various azimuths.

3.2 ANALYSIS APPROACH

The basic steps required to analyze the configuration in Figure 3-1 is as follows:

1. Choose basic system components and determine the zero current equilibrium configuration.
2. Analyze the response of the two vertical strings relative to their connection point on the array. Since the vertical strings have a free end their relative motion will be independent of the movement of the trapezoid. This is strictly true for uniform currents and may or may not be true for current profiles. The latter case is dependent on the vertical response of the trapezoid in that it may position the vertical string in a different current regime.
3. The analysis of (1) will output a tension vector at the trapezoid apex which will be used in the trapezoidal configuration analysis.
4. Analyze the trapezoidal array using Newtons method (described in Appendix B) to determine the static response configuration.

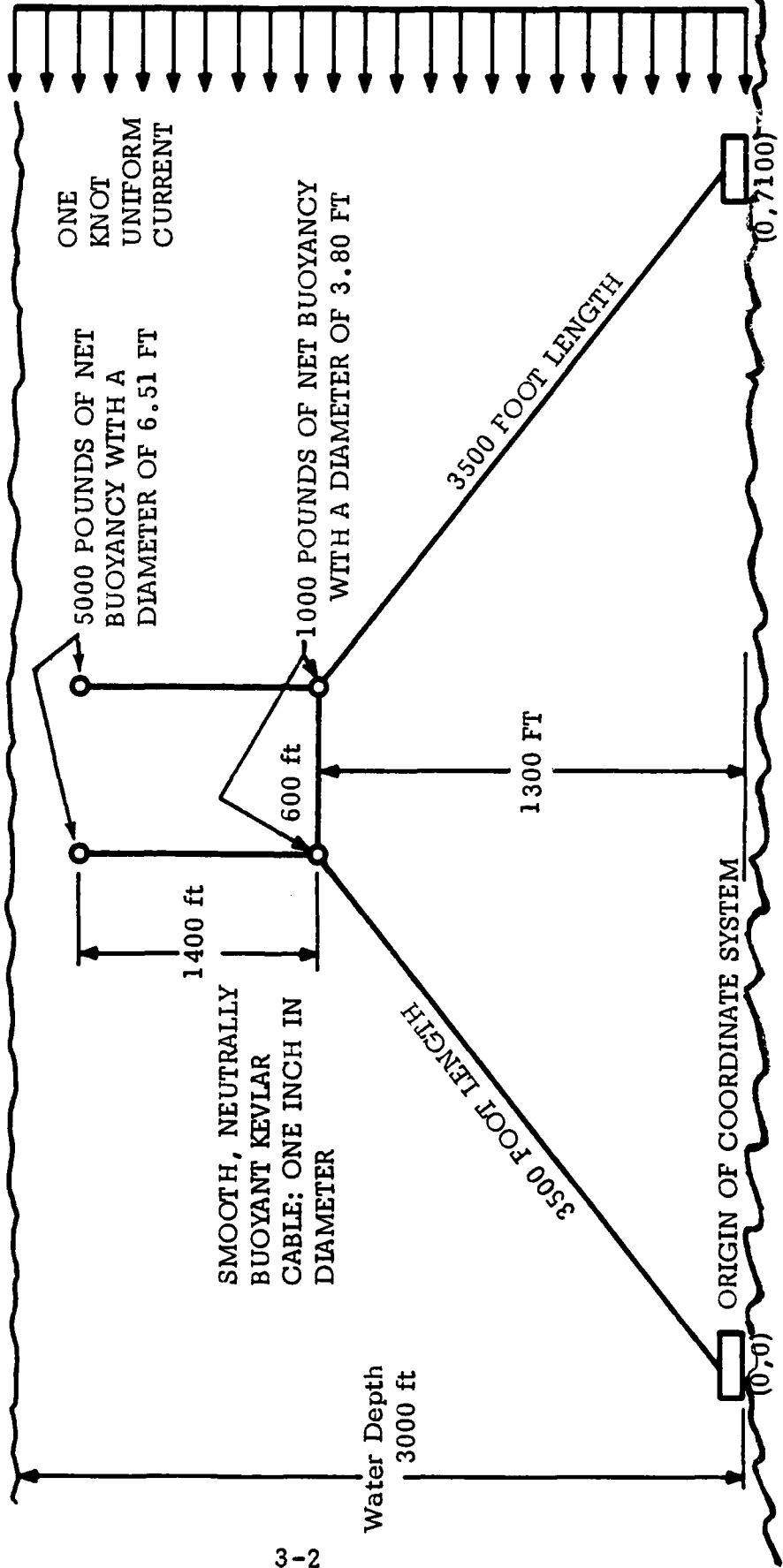


Figure 3-1. Far-Field Goal Post Array Analysis Diagram

5. Combine the geometry response of the vertical strings and the trapezoid to obtain the overall response of the vertical string top buoy which is to remain as stationary as possible.

The following sections discuss the specifics of each step discussed above.

3.3 BASIC CONFIGURATION

Figure 3-2 depicts the equilibrium diagram for the zero current case that has been assumed for illustrative purposes. The forces and angles result from straightforward calculations. The trapezoidal cables are straight lines since it is assumed that they are neutrally buoyant with no hydrodynamic forces present from currents.

3.4 ANALYSIS OF VERTICAL STRINGS

The vertical strings were analyzed parametrically for various buoys, cable diameters and current velocities. The resultant watch circle data represents a "best case" in total watch circle response, because it assumes the trapezoid to be stationary. Figure 3-3 depicts the parameters assumed for the analysis. The technique is similar to that used on the near field array and discussed in Section 2.

Table 3-1 contains the analytical results in terms of watch circle radius and vertical displacement of the top buoy relative to the connection point at the apex of the trapezoid. Figure 3-4 graphically depicts the same results. Note that the design goal of 3-foot watch circle radius is highlighted and eliminates the majority of configurations examined.

For purposes of the goal post array system analysis the solution using a 5000 lb. buoy and a 1.0 inch diameter Kevlar cable in a 1-knot current was used. From the analysis of this case the vertical string tension at the trapezoid was 5997.42 lbs. tension at an angle of 95.33° degrees.

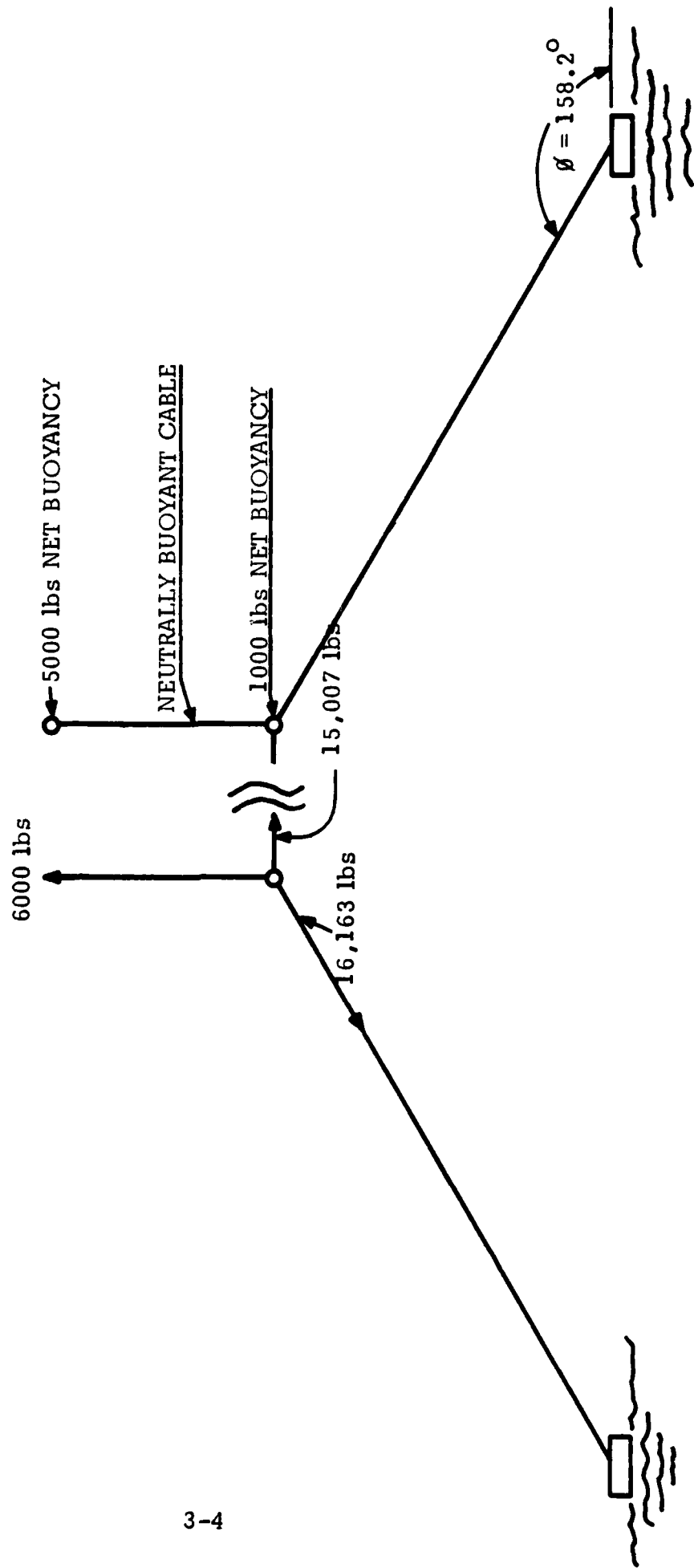


Figure 3-2. Equilibrium Diagram for the Trapezoidal Array
With Zero Current

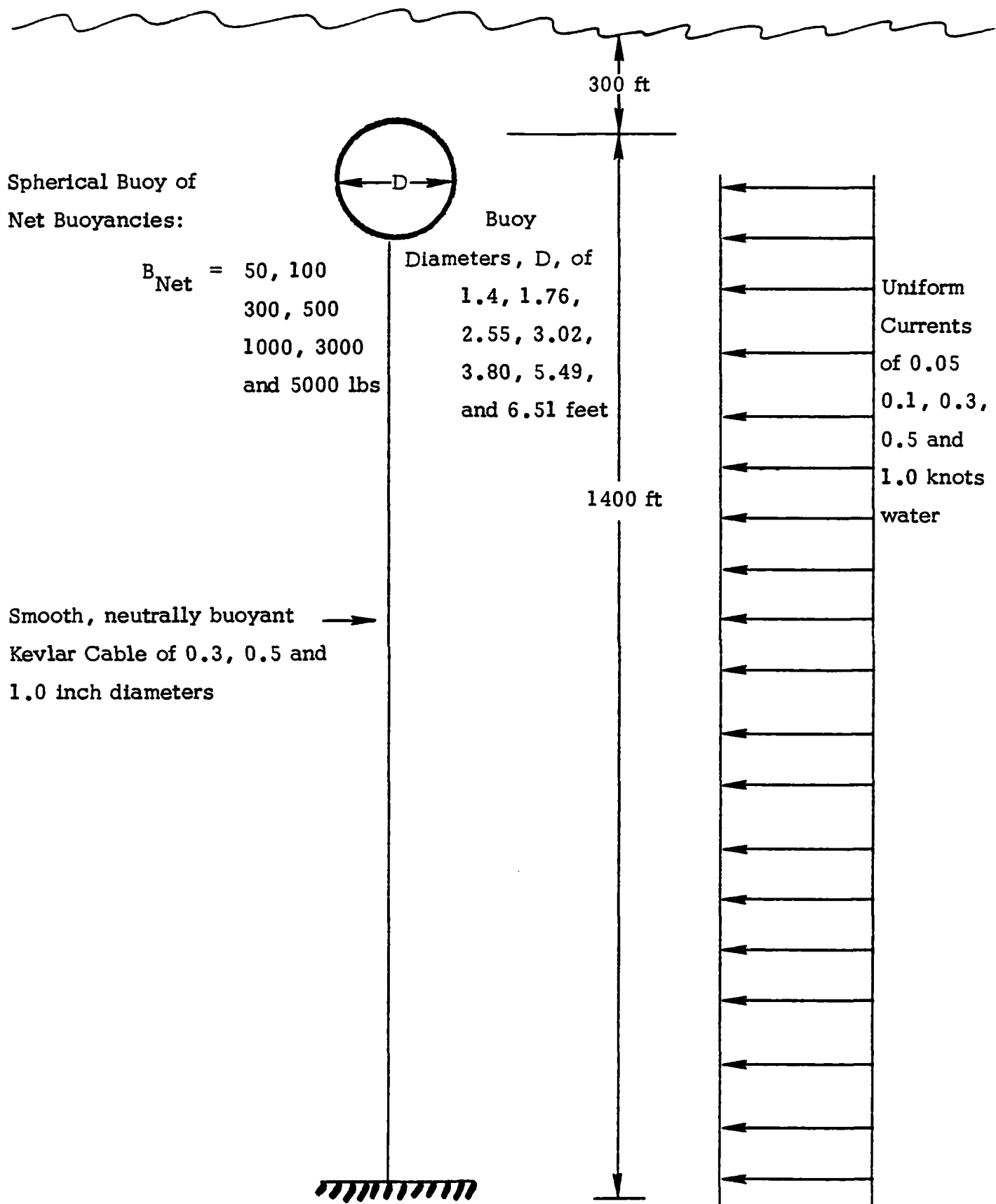


Figure 3-3. Vertical Strings Analysis Diagram

PRELIMINARY WATCH CIRCLE TRADE-OFFS OF VERTICAL SENSOR STRINGS

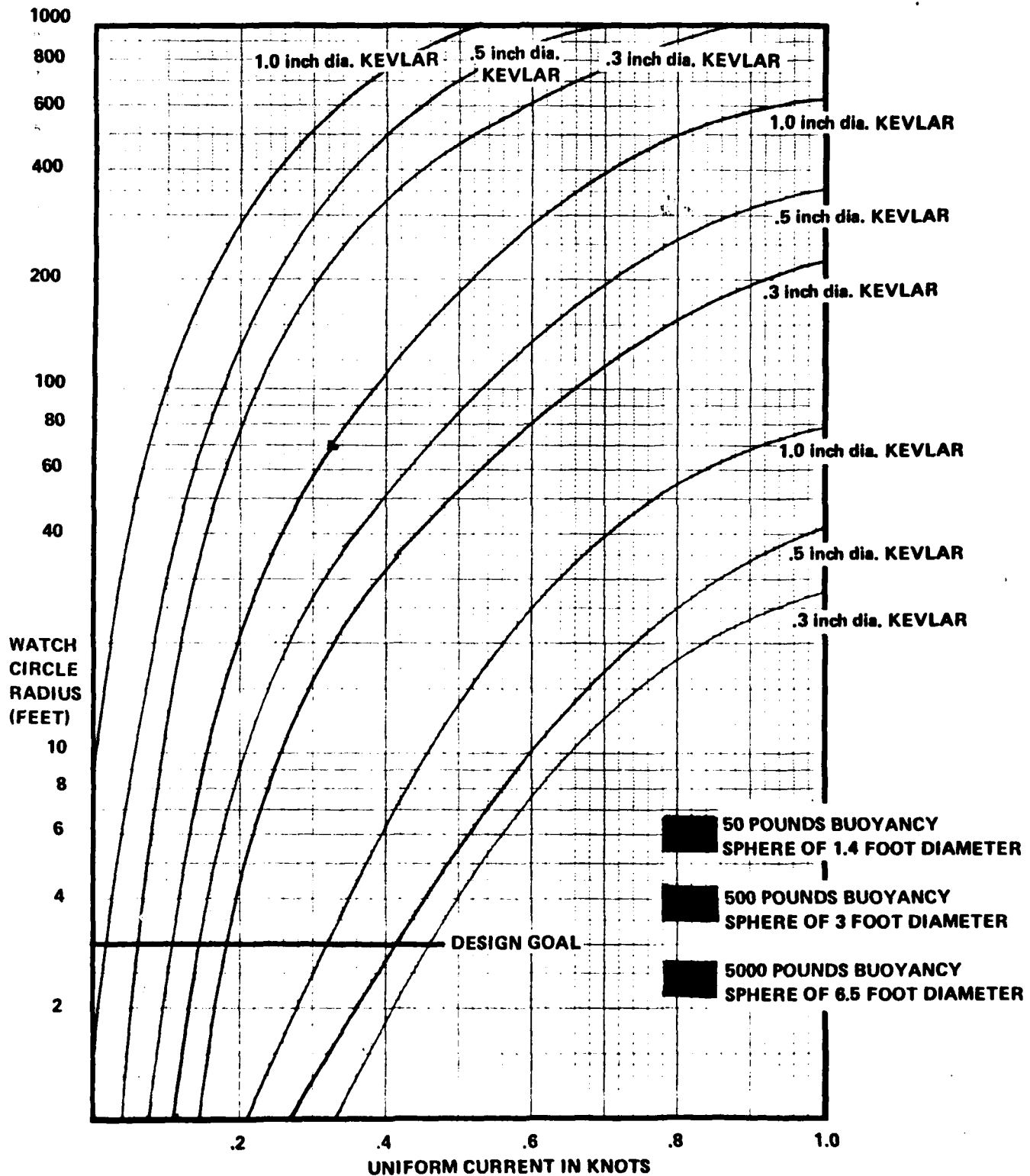


Figure 3-4. Preliminary Watch Circle Trade-offs of Vertical Sensor Strings

Table 3-1. Geometric Response for Vertical Strings for Various Combinations of Buoyancy, Cable Diameter, and Uniform Current

.05 KNOT CURRENT				0.10 KNOT CURRENT			
Net Buoyancy (Pounds)	Cable Diameter (Inches)	Displacement In X Watch Radius	Displacement In Y Dip	Net Buoyancy (Pounds)	Cable Diameter (Inches)	Displacement In X Watch Radius	Displacement In Y Dip
50	.3	0.17	0.00	50	.3	14.54	0.12
	.5	2.90	0.01		.5	28.44	0.43
	1.0	11.27	0.08		1.0	63.13	1.99
100	.3	0.13	0.00	100	.3	5.10	0.02
	.5	0.13	0.00		.5	11.59	0.09
	1.0	2.86	0.01		1.0	28.32	0.43
300	.3	0.44	0.00	300	.3	0.34	0.00
	.5	0.09	0.00		.5	0.34	0.00
	1.0	0.09	0.00		1.0	5.89	0.03
500	.3	0.28	0.00	500	.3	0.29	0.00
	.5	0.43	0.00		.5	0.29	0.00
	1.0	0.07	0.00		1.0	0.29	0.00
1000	.3	0.16	0.00	1000	.3	0.23	0.00
	.5	0.23	0.00		.5	0.23	0.00
	1.0	0.41	0.00		1.0	0.23	0.00
3000	.3	0.09	0.00	3000	.3	0.30	0.00
	.5	0.10	0.00		.5	0.39	0.00
	1.0	0.16	0.00		1.0	0.16	0.00

Table 3-1. Geometric Response for Vertical Strings for Various Combinations of Buoyancy, Cable Diameter, and Uniform Current (cont.)

Net Buoyancy (Pounds)	0.3 KNOT CURRENT			0.5 KNOT CURRENT			
	Cable Diameter (Inches)	Displacement In X Watch Radius	Displacement In Y Dip	Net Buoyancy (Pounds)	Cable Diameter (Inches)	Displacement In X Watch Radius	Displacement In Y Dip
50	.3	183.69	16.20	50	.3	475.47	109.73
	.5	299.30	43.25		.5	682.91	233.53
	1.0	539.43	143.71		1.0	958.24	490.69
100	.3	91.05	4.01	100	.3	258.45	31.77
	.5	152.33	11.17		.5	406.99	79.98
	1.0	298.23	43.02		1.0	680.90	232.55
300	.3	27.74	0.39	300	.3	88.25	3.68
	.5	48.41	1.16		.5	145.15	10.01
	1.0	100.01	4.86		1.0	281.38	37.99
500	.3	14.92	0.12	500	.3	52.48	1.31
	.5	27.26	0.38		.5	86.93	3.60
	1.0	58.15	1.67		1.0	191.90	14.12
1000	.3	5.60	0.02	1000	.3	56.65	1.47
	.5	11.26	0.08		.5	91.09	3.86
	1.0	26.73	0.37		1.0	175.98	14.63
3000	.3	1.41	0.00	3000	.3	6.65	0.03
	.5	1.42	0.00		.5	11.64	0.07
	1.0	6.02	0.00		1.0	26.11	0.34
5000	.3	1.19	0.00	5000	.3	3.31	0.00
	.5	1.19	0.00		.5	6.04	0.02
	1.0	1.20	0.00		1.0	14.41	0.11

Table 3-1. Geometric Response for Vertical Strings for Various Combinations of Buoyancy, Cable Diameter, and Uniform Current (cont.)

1.0 KNOT CURRENT			
Net Buoyancy (Pounds)	Cable Diameter (Inches)	Displacement In X Watch Radius	Displacement In Y Dip
50	.3	1032.75	575.45
	.5	1165.32	781.01
	1.0	1278.33	1013.63
100	.3	777.65	303.36
	.5	970.22	499.01
	1.0	1162.96	799.03
300	.3	354.94	58.76
	.5	530.37	135.42
	1.0	812.77	336.83
500	.3	225.60	23.30
	.5	350.20	57.56
	1.0	599.06	175.59
1000	.3	241.55	25.97
	.5	365.02	61.27
	1.0	610.70	180.65
3000	.3	43.50	0.81
	.5	66.71	1.99
	1.0	123.95	7.08
5000	.3	27.15	.31
	.5	41.05	.74
	1.0	75.69	2.62

3.5 DETERMINE RESULTANT FORCE ON TRAPEZOID

In addition to the vertical string tension vector it was assumed that a 1000 lb. buoy was located at each trapezoid apex. Figure 3-5 depicts the vector force diagram that computes the resultant force acting on the trapezoid.

3.6 ANALYSIS OF THE TRAPEZOID

The application of Newton's method in calculating the catenary of the goal post configuration current response consists of utilizing the known zero current geometry of the goal post array and utilizing the catenary computer program to successively calculate trial solutions. The process is started by (1) assuming a new tension vector at the base of the trapezoid; (2) assuming a perturbed set of tension vectors about that chosen in (1); (3) calculating the resultant catenary of the trapezoid; (4) comparing the catenary results to the compatibility equations; (5) predicting the next initial condition from the error derivatives; and (6) computing the system watch circles. The following example illustrates this procedure whose theoretical approach is detailed in appendix B.

3.6.1 Assume a New Tension Vector

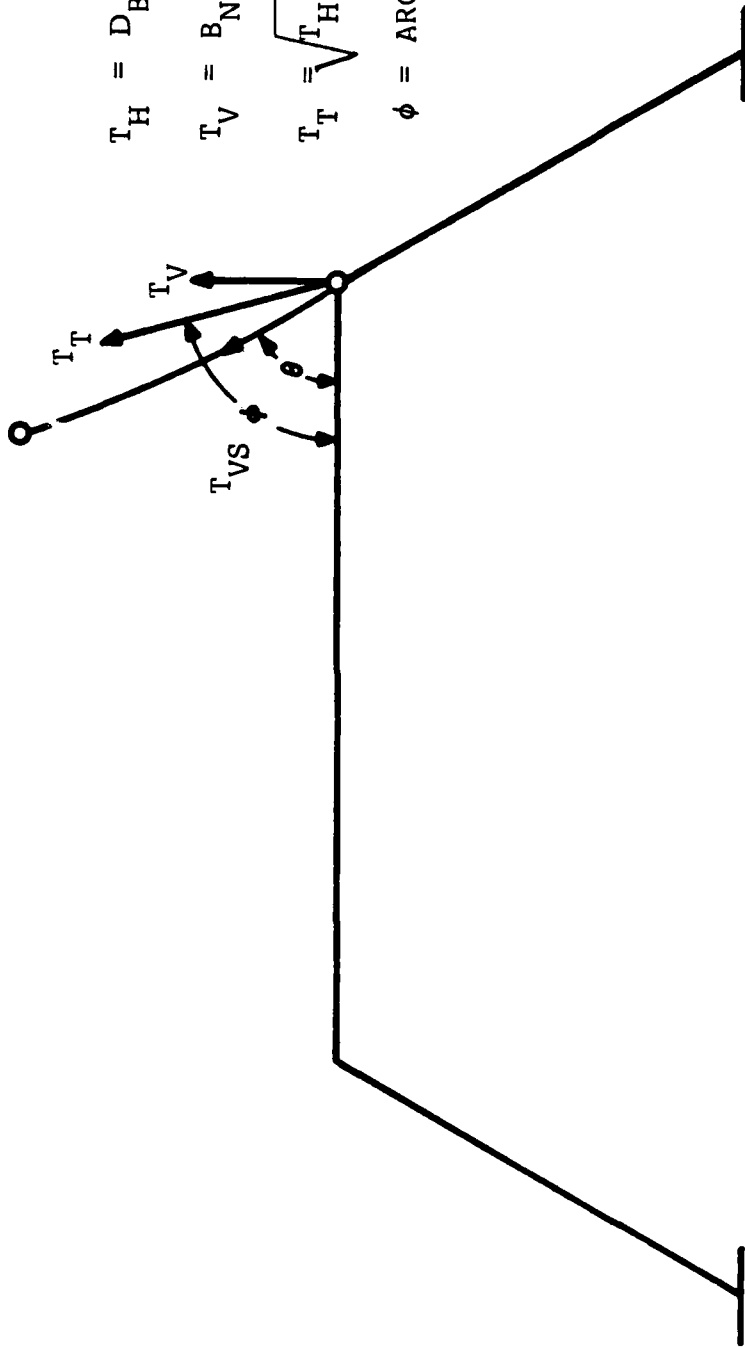
Figure 3-6 depicts an intuitive response geometry to the trapezoid from an imposed current. The tension will increase and the angle will increase at Point A. Therefore, an assumed solution is:

$$T_1 = 16,200 \text{ lbs } (T_0 \text{ was } 16,163.57)$$

$$\theta_1 = 159.0 \text{ degrees } (\theta_0 \text{ was } 158.19)$$

3.6.2 Assume a Perturbed Set of Initial Conditions

The purpose of this is to find the effect of small perturbations of the assumed solution on the compatibility relationships in order to form error derivatives.



$$T_H = D_B + T_{VS} \cos \theta$$

$$T_V = B_N + T_{VS} \sin \theta$$

$$T_T = \sqrt{T_H^2 + T_{VS}^2}$$

$$\phi = \text{ARCTAN } T_V/T_H$$

Figure 3-5. Vector Force Diagram For Determining Resultant Force on Trapezoid Apex.

ZERO CURRENT CONDITION
INTUITIVE RESPONSE TO CURRENT

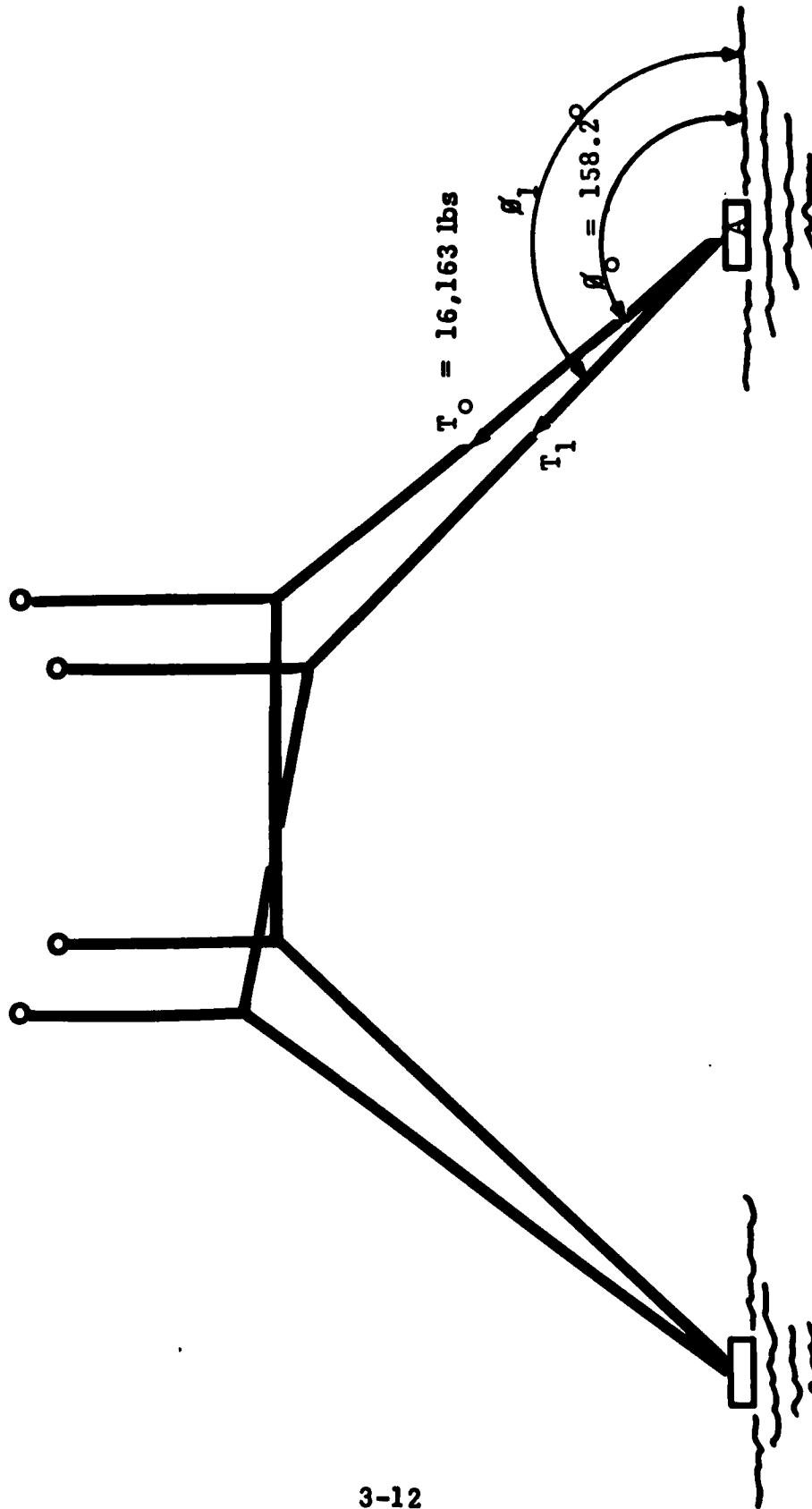


Figure 3-6. Intuitive Response Geometry to a Planar Current for the Goal Post Array

For purposes of this example the two sets are:

$$\left. \begin{aligned} T_1 + \Delta T &= 16,200 + 5 = 16,205 \text{ lbs} \\ \theta_1 &= \theta_1 = 159 \text{ degrees} \end{aligned} \right\}$$

$$\left. \begin{aligned} T_1 &= T_1 = 16,200 \text{ lbs} \\ \theta_1 + \Delta\theta &= 159 + (0.1) = 159.1 \text{ degrees} \end{aligned} \right\}$$

3.6.3 Calculate the Resultant Catenary of the Trapezoid

Using the three sets of initial conditions:

$$T_1, \theta_1,$$

$$T_1 + \Delta T, \theta_1$$

$$T, \theta_1 + \Delta\theta$$

The resultant geometry of the end of the trapezoid relative to the known coordinates of the end point (0,0) are: (See Figure 3-7)

Initial Condition	f	g
$\left. \begin{aligned} T_1 &= 16,200 \text{ lbs} \\ \theta_1 &= 159^\circ \end{aligned} \right\}$	23.24	-137.78
$\left. \begin{aligned} T_1 &= 16,205 \text{ lbs} \\ \theta_1 &= 159^\circ \end{aligned} \right\}$	22.90	-136.95
$\left. \begin{aligned} T_1 &= 16,200 \text{ lbs} \\ \theta_1 &= 159.1^\circ \end{aligned} \right\}$	22.94	-149.29

3.6.4 Compute Errors from the Compatibility Relationships

From the known relative geometry of the anchor points of the trapezoid the following conditions must hold (refer to Figure 3-7):

$$f = X = 0$$

$$g = y = 0$$

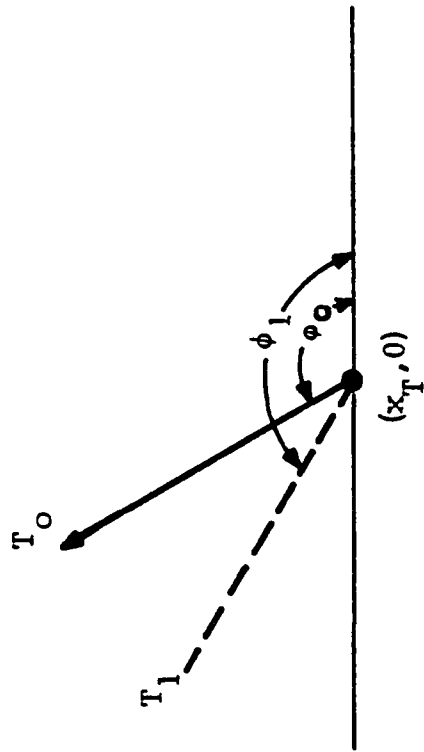
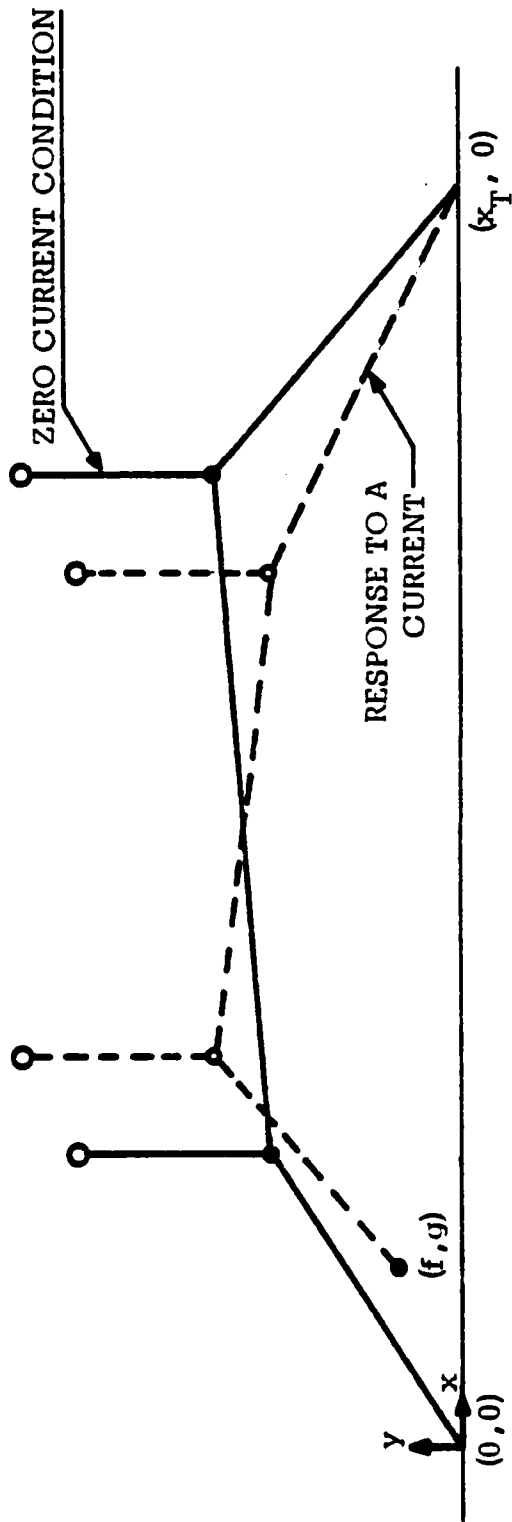


Figure 3-7. Trapezoidal Array Nomenclature

For the cases above the error derivatives are: (see Appendix B for derivatives)

$$\frac{\partial f}{\partial T} = \frac{22.90 - 23.24}{16,205 - 16,200} = -0.068$$

$$\frac{\partial f}{\partial \theta} = \frac{22.94 - 23.24}{159.1 - 159} = -3.00$$

$$\frac{\partial g}{\partial T} = \frac{-136.95 - (-137.78)}{16,205 - 16,200} = 0.166$$

$$\frac{\partial g}{\partial \theta} = \frac{-149.29 - (-137.78)}{159.1 - 159} = -115.10$$

3.6.5 Predict the Next Initial Condition for T and θ in Order for $f = g = 0$

The next set of conditions are:

$$T_2 = T_1 + dT$$

$$\theta_2 = \theta_1 + d\theta$$

$$\text{where } T_1 = 16,200 \text{ lbs} \quad \theta_1 = 159^\circ$$

$$dT = - \left[\frac{f \frac{\partial g}{\partial \theta} - g \frac{\partial f}{\partial \theta}}{\frac{\partial f}{\partial T} \frac{\partial g}{\partial \theta} - \frac{\partial g}{\partial T} \frac{\partial f}{\partial \theta}} \right] \text{ and}$$

$$d\theta = - \left[\frac{\frac{\partial f}{\partial T} g - f \frac{\partial g}{\partial T}}{\frac{\partial f}{\partial T} \frac{\partial g}{\partial \theta} - \frac{\partial g}{\partial T} \frac{\partial f}{\partial \theta}} \right]$$

Using the numbers calculated in section 3.6.4 the new assumptions for T and θ are:

$$\begin{aligned} T_2 &= 16,200 - \left[\frac{(23.24) (-115.10) - (-137.78) (-3.00)}{(-0.068) (-115.10) - (0.166) (-3.00)} \right] \\ &= 16,200 + 370.97 = 16,570.97 \end{aligned}$$

$$\begin{aligned} \theta_2 &= 159 + \frac{(-137.78)(-0.068) - (23.24)(0.166)}{(-0.068)(-115.1) - (0.166)(-3.00)} \\ &= 159 - 0.66 = 158.34 \end{aligned}$$

A new set of perturbed conditions about T_2 , θ_2 were computed and the process continued. After a total of three iterations, the following results were obtained for a 1 knot uniform current:

<u>Scope (ft)</u>	<u>X (ft)</u>	<u>Y (ft)</u>	<u>Tension (lb)</u>	<u>θ (degrees)</u>
0	7100.00	0	16,597.46	158.38
3500	3847.55	1292.85	16,561.21	157.74
3500	3847.55	1292.85	14,772.90	178.85
4100	3247.67	1304.90	14,770.65	178.85
4100	3247.67	1304.90	15,303.77	158.21
7600	0.06	-0.02	15,267.23	157.51

The above data can be compared to the zero current case presented below:

<u>Scope (ft)</u>	<u>X (ft)</u>	<u>Y (ft)</u>	<u>Tension (lbs)</u>	<u>θ (degrees)</u>
0	7100.00	0	16163.6	158.19
3500	3850.00	1300.00	16163.6	158.19
3500	3850.00	1300.00	15006.6	180.00
4100	3250.00	1300.00	15006.6	180.00
4100	3250.00	1300.00	16163.6	158.19
7600	0	0	16163.6	158.19

3.6.6 Compute the System Watch Circles

The resultant watch circle of the various parts of the goal post array system are computed below:

- Displacement of Buoy "A" in a 1 knot current relative to a zero current condition:
 - x displacement: $3847.55 - 3850 = -2.45$ ft
 - y displacement: $1292.85 - 1300 = -7.15$ ft

- Displacement of Buoy "B" in a 1 knot current relative to a zero current condition:

$$x \text{ displacement: } 3247.67 - 3250 = -2.33 \text{ ft}$$

$$y \text{ displacement: } 1304.90 - 1300 = 4.90 \text{ ft}$$

- Displacement of Vertical string buoy "C" relative to buoy "A" and buoy "D" relative to buoy "B":

$$\left. \begin{array}{l} x \text{ displacement} = 75.69 \text{ ft} \\ y \text{ displacement} = -2.62 \text{ ft} \end{array} \right\} \text{ From Table 3-1}$$

- Total displacement of buoy "C":

$$x \text{ displacement} = -75.69 - 2.45 = -78.14$$

$$y \text{ displacement} = -2.62 - 7.15 = -9.77 \text{ (dip)}$$

- Total displacement of buoy "D":

$$x \text{ displacement} = -75.69 - 2.33 = -78.02$$

$$y \text{ displacement} = -2.62 + 4.90 = 2.28 \text{ (rise)}$$

3.7 OBSERVATIONS OF FAR-FIELD GOAL POST ANALYSIS

The analysis presented in the preceding sections have demonstrated a method of assessing the array response to the environmental effects of current. It is apparent from the analysis of the vertical strings (Figure 3-4) that watch circles in the order of 3 ft. can only be maintained under very low current conditions (.4 knots or less depending on buoyancy and size of cable). The analysis model presented herein has been intended to demonstrate an approach for estimating array response to ocean currents. Definition of system components and in-situ current profiles are needed to provide more accurate results; however, the model should be used in a parametric sense to assist in arriving at a final design. Finally the model can be easily extended to examine non-planar currents for a total excursion analysis capability.

Appendix A
CALCULATIONS
OF SPHERICAL BUOY
PARAMETERS

The buoyant member was assumed to be a spherical buoy made of 6061-T6 aluminum with a 3000 foot working depth and a design safety factor of 3.

Computations were made to determine the wall thickness versus the inner and outer radius of the spherical buoy. An incremental element of stress was defined as

$$\sigma = q R_2 / 2 t$$

where q = the external pressure

R_2 = the inner wall radius of the buoy

t = the buoy wall thickness

and $q = \rho g h$

$$= \frac{(1.99 \text{ slug/foot}^3) (32.2 \text{ ft/sec}^2) (3000 \text{ feet})}{144 \text{ inch}^2/\text{foot}^2}$$

$$= 1335 \text{ p.s.i.}$$

The maximum allowable stress is given by

$$\sigma \text{ max} = \frac{\text{Compressive Yield Strength of Material}}{\text{Safety Factor}}$$

For 6061-T6 aluminum the compressive yield strength is 35,000 psi. Therefore

$$\sigma_{\max} = \frac{35000}{3} = 11667 \text{ psi}$$

Thus

$$\sigma_{\max} = qR_2/2t$$

$$R_2/t = 2(11667)/1135 = 17.5$$

Since

$$R_2 = R - t/2$$

where R = the outer radius of
the buoy

Then

$$\frac{R - t/2}{t} = 17.5$$

$$R = 17.5t + t/2$$

$$R/t = 18$$

Calculations were then made of the net buoyancy versus radius. Since the net buoyancy,

$$B_{\text{net}} = B_{\text{gross}} - \text{Weight of the buoy}$$

Then

$$\begin{aligned} B_{\text{net}} &= \frac{4}{3} \pi R^3 \gamma_{\text{water}} - \left[\frac{4}{3} \pi R^3 \gamma_{\text{al}} - \frac{4}{3} \pi (R-t)^3 \gamma_{\text{al}} \right] \\ &= \frac{4}{3} \pi \left[R^3 (\gamma_{\text{water}} - \gamma_{\text{al}}) - (R-t)^3 \gamma_{\text{al}} \right] \end{aligned}$$

$$\text{Since } R/t = 18$$

$$\begin{aligned} B_{\text{net}} &= \frac{4}{3} \pi \left[R^3 (\gamma_{\text{water}} - \gamma_{\text{al}}) - (R - R/18)^3 \gamma_{\text{al}} \right] \\ &= \frac{4}{3} \pi \left[R^3 (\gamma_{\text{water}} - \gamma_{\text{al}}) - 1.176 R^3 \gamma_{\text{al}} \right] \\ &= \frac{4}{3} \pi R^3 (\gamma_{\text{water}} - 0.1761 \gamma_{\text{al}}) \end{aligned}$$

$$\text{Since } \gamma_{\text{water}} = 64.4 \text{ lb/ft}^3$$

$$\gamma_{\text{al}} = 169.3 \text{ lb/ft}^3$$

$$B_{\text{net}} = 144.8 R^3$$

where R is in feet

Subsequently Table A-1 presents the buoyancies examined versus the outside diameter of the aluminum spheres required to produce such buoyancy.

Table A-1 Net Buoyancy and Buoy Diameter

B(net) (lbs)	Diameter (feet)
50	1.40
100	1.76
300	2.55
500	3.02
1000	3.80
3000	5.49
5000	6.51

The semifixed array was evaluated in uniform currents of 0.05, 0.1, 0.3, 0.5, and 1.0 Knots. Consequently the drag, D, caused by the buoy was computed by

$$D = C_D A (1/2 \rho V^2)$$

where C_D = drag coefficient

$$= .5 \text{ for } 10^3 < Re < 3 \times 10^5$$

A = spherical area

$$= \pi D^2/4$$

ρ = Density of Water

$$= 1.99 \text{ slugs}$$

$$V^2 = \text{Velocity in Knots}^2 \left(1.689 \frac{\text{ft/sec}}{\text{kt}} \right)^2$$

Table A-2
Spherical Buoy Drag, lbs

Net Buoyancy lbs.	Current Velocity, Kts.				
	0.05	0.1	0.3	0.5	1.0
50	.006	.022	.197	.546	2.18
100	.009	.035	.311	.863	3.45
300	.018	.073	.652	1.812	7.25
500	.025	.102	.916	2.545	10.18
1000	.040	.162	1.455	4.041	16.16
3000	.084	.336	3.036	8.405	33.62
5000	.118	.473	4.254	11.82	47.27

Appendix B

APPLICATION OF NEWTON'S METHOD IN CALCULATING THE EQUILIBRUM CONFIGURATION OF A TWO-LEGGED BUOY MOORING WITH AN IN PLANE CURRENT

Newton's method is basically a numerical iterative means for finding a zero of a function $f(x)$. This method can be extended to mathematical systems of n equations in n unknowns.

For application to the trapezoidal array reference is made to Figure B-1. In order to calculate an assumed configuration due to a current a new tension vector at point $(X_T, 0)$ is assumed and the resultant location of the end point (f, g) determines how accurate your initial assumption was. In order for your assumption to be correct:

$$f = g = 0 \quad (\text{B-1})$$

The total differential of f and g can be expressed as:

$$df = \frac{\partial f}{\partial T} dT + \frac{\partial f}{\partial \theta} d\theta = \cancel{f_2}^0 - f_1 \quad (\text{B-2})$$

$$dg = \frac{\partial g}{\partial T} dT + \frac{\partial g}{\partial \theta} d\theta = \cancel{g_2}^0 - g_1 \quad (\text{B-3})$$

In order for f_2 and g_2 to be equal to zero, the following expression in matrix form must hold:

$$\begin{bmatrix} \frac{\partial f}{\partial T} & \frac{\partial f}{\partial \theta} \\ \frac{\partial g}{\partial T} & \frac{\partial g}{\partial \theta} \end{bmatrix} \begin{bmatrix} dT \\ d\theta \end{bmatrix} = \begin{bmatrix} -f_1 \\ -g_1 \end{bmatrix} \quad (\text{B-4})$$

or,

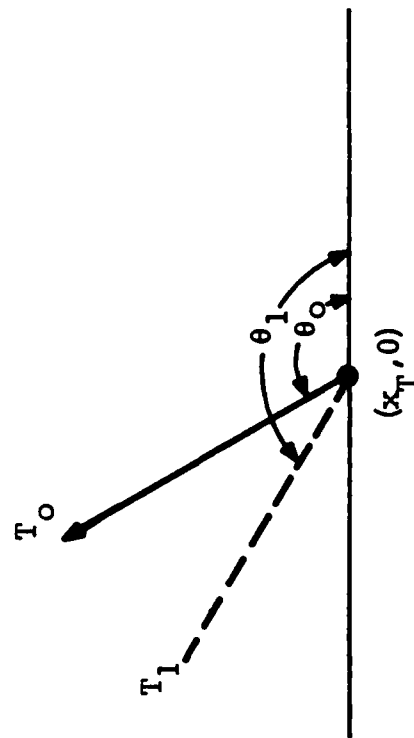
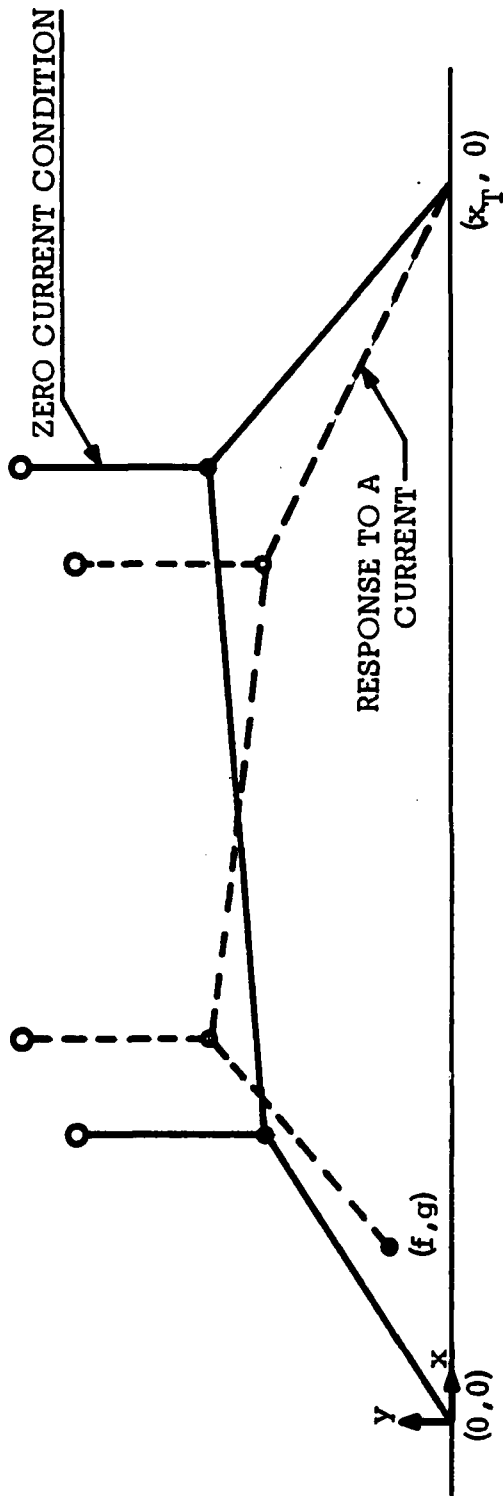


Figure B-1. Trapezoidal Array Nomenclature

$$d\theta = - \left[\frac{\frac{\partial f}{\partial T} g - f \frac{\partial g}{\partial T}}{\frac{\partial f}{\partial T} \frac{\partial g}{\partial \theta} - \frac{\partial f}{\partial \theta} \frac{\partial g}{\partial T}} \right] \quad (B-5)$$

$$dT = - \left[\frac{f \frac{\partial g}{\partial \theta} - g \frac{\partial f}{\partial \theta}}{\frac{\partial f}{\partial T} \frac{\partial g}{\partial \theta} - \frac{\partial f}{\partial \theta} \frac{\partial g}{\partial T}} \right] \quad (B-6)$$

Therefore the next choice for T_2 and θ_2 in order to make $f_2 = g_2 = 0$ are:

$$T_2 = T_1 + dT \quad (B-7)$$

$$\theta_2 = \theta_1 + d\theta \quad (B-6)$$

where dT and $d\theta$ are defined in equations B-6 and B-5 respectively.

The error derivatives $\frac{\partial f}{\partial T}$, $\frac{\partial g}{\partial T}$, $\frac{\partial f}{\partial \theta}$, and $\frac{\partial g}{\partial \theta}$ are evaluated by obtaining values of f and g for very small variations of the initial assumption T_1, θ_1 , that is:

$$\frac{\partial f}{\partial T} = \frac{f_{(T_1 + \Delta T), \theta_1} - f_{(T_1, \theta_1)}}{\Delta T} \quad (B-7)$$

$$\frac{\partial g}{\partial T} = \frac{g_{(T_1 + \Delta T), \theta_1} - g_{(T_1, \theta_1)}}{\Delta T} \quad (B-8)$$

$$\frac{\partial f}{\partial \theta} = \frac{f_{(T_1, \theta_1 + \Delta \theta)} - f_{(T_1, \theta_1)}}{\Delta \theta} \quad (B-9)$$

$$\frac{\partial g}{\partial \theta} = \frac{g_{(T_1, \theta_1 + \Delta \theta)} - g_{(T_1, \theta_1)}}{\Delta \theta} \quad (B-10)$$

The solution will converge quadratically and as in the example presented in Section 3, takes about 4 iterations in order to obtain $f = g \approx 0$.

END

DTIC

4-86